

**Immunological characterization of two types of ionocytes in the inner ear epithelium of Pacific Chub Mackerel (*Scomber japonicus*)**

Garfield T. Kwan, Taylor R. Smith, Martin Tresguerres\*

Marine Biology Research Division, Scripps Institution of Oceanography, University of California San Diego

\*Corresponding author: mtresguerres@ucsd.edu

**Abstract:**

The inner ear is essential for maintaining balance and hearing predator and prey in the environment. Each inner ear contains three  $\text{CaCO}_3$  otolith polycrystals, which are calcified within an alkaline,  $\text{K}^+$ -rich endolymph secreted by the surrounding epithelium. However, the underlying cellular mechanisms are poorly understood, especially in marine fish. Here, we investigated the presence and cellular localization of several ion-transporting proteins within the saccular epithelium of the Pacific Chub Mackerel (*Scomber japonicus*). Western blotting revealed the presence of  $\text{Na}^+/\text{K}^+$ -ATPase (NKA), carbonic anhydrase (CA),  $\text{Na}^+/\text{K}^+/\text{2Cl}^-$ -co-transporter (NKCC), vacuolar-type  $\text{H}^+$ -ATPase (VHA), plasma membrane  $\text{Ca}^{2+}$  ATPase (PMCA), and soluble adenylyl cyclase (sAC). Immunohistochemistry analysis identified two distinct ionocytes types in the saccular epithelium: Type-I ionocytes were mitochondrion-rich and abundantly expressed NKA and NKCC in their basolateral membrane, indicating a role in secreting  $\text{K}^+$  into the endolymph. On the other hand, Type-II ionocytes were enriched in cytoplasmic CA and VHA, suggesting they help transport  $\text{HCO}_3^-$  into the endolymph and remove  $\text{H}^+$ . Additionally, both types of ionocytes expressed cytoplasmic PMCA, which is likely involved in  $\text{Ca}^{2+}$  transport and homeostasis, as well as sAC, an evolutionary conserved acid-base sensing enzyme that regulates epithelial ion transport. Furthermore, CA, VHA, and sAC were also expressed within the capillaries that supply blood to the meshwork area, suggesting additional mechanisms that contribute to otolith calcification. This information improves our knowledge about the cellular mechanisms responsible for endolymph ion regulation and otolith formation, and can help understand responses to environmental stressors such as ocean acidification.

**Key Words (up to 6 words, listed alphabetically):** ATPase, biomineralization, calcification, ocean acidification, otolith, soluble adenylyl cyclase

## Introduction

The inner ear senses gravity and sound waves, which is essential for maintaining balance and hearing predator and prey in the environment (Dijkgraaf, 1960; Furukawa and Ishii, 1967; reviewed in Ladich and Schulz-Mirbach, 2016). Enclosed within each inner ear are the sagittal, lapilli, and asterisci otoliths, which are composed of a protein matrix and calcium carbonate ( $\text{CaCO}_3$ ). The higher density of the otolith compared to the inner ear fluid (“endolymph”) results in differential inertia that stimulates the adjacent sensory hair cells, which the brain interprets as soundwaves or movement.

Being the largest of the three otoliths, the sagitta and its surrounding saccular epithelium have been most extensively studied. The saccular epithelium has been previously characterized as the macula, meshwork, patches, and intermediate areas (Mayer-Gostan et al., 1997; Pisam et al., 1998). The macula contains the sensory hair cells that detect otolith vibration and movement. This area is flanked by the meshwork area, which contains large ion-transporting cells (“ionocytes”). The patches area is positioned directly across from the macula and contains patches of smaller ionocytes. The intermediate area is largely devoid of ionocytes, but does contain some ionocytes in the area bordering the meshwork area and smaller ionocytes bordering the patches area. Each otolith is calcified within an alkaline,  $\text{K}^+$ -rich endolymph secreted by its respective saccule, utricle and lagena inner ear epithelium.

In the Rainbow Trout (*Oncorhynchus mykiss*), the endolymph has a pH of  $\sim 8$ ,  $\sim 30$  mmol of  $\text{HCO}_3^-$ ,  $\sim 124$  mmol of  $\text{K}^+$ ,  $\sim 90$  mmol of  $\text{Na}^+$ , and  $\sim 1.1$  mmol of  $\text{Ca}^{2+}$  (Payan et al., 1997). When compared to its blood plasma, the endolymph is roughly 0.8 pH unit higher, has twice as much  $\text{HCO}_3^-$ ,  $\sim 40$ -fold higher  $\text{K}^+$ , half as much  $\text{Na}^+$ , and twice as much  $\text{Ca}^{2+}$  (Payan et al., 1997). This dramatic differences between the endolymph and blood plasma are thought to be attributed to the surrounding ionocytes’ activity. To date, two different types of ionocytes have been characterized: one is mitochondrion-rich (MR), has well-developed basolateral membrane infoldings (Mayer-Gostan et al., 1997), and abundantly expresses  $\text{Na}^+/\text{K}^+$ -ATPase (NKA) (Takagi, 1997), whereas the other one has abundant cytoplasmic carbonic anhydrase (CA) (Tohse et al., 2004, 2006). The NKA-rich ionocytes are proposed to be responsible for transporting  $\text{K}^+$  (Payan et al., 1999),  $\text{Ca}^{2+}$  (Mugiya and Yoshida, 1995) and removing  $\text{H}^+$  (Payan et al., 1997) from the endolymph, whereas the CA-rich ionocytes are thought to transport  $\text{HCO}_3^-$ .

into the endolymph (Tohse and Mugiya, 2001; reviewed in Payan et al., 2004). These models would imply the NKA-rich ionocytes should have different ion-transporting proteins than the CA-rich ionocytes.

Moreover, the endolymph's composition is not homogeneous (Payan et al., 1999; Borelli et al., 2003). The proximal endolymph, which is located between the otolith and the macula and meshwork area, has lower  $[K^+]$  and total  $CO_2$  compared to the distal endolymph, which is located between the other side of the otolith and the intermediate and patches area (Payan et al., 1999). Though  $[Ca^{2+}]$  does not differ between the proximal and distal endolymph (Payan et al., 1999; Borelli et al., 2003), the proximal endolymph has a 3-fold higher concentration of glycoprotein (Payan et al., 1999), which may chelate  $Ca^{2+}$  and catalyze aragonite crystallization (Murayama et al., 2002; Ibsch et al., 2004). Correspondingly, the otolith's proximal surface calcifies faster than the distal surface (Payan et al., 1999; Borelli et al., 2003; Beier et al., 2006). And although it was not directly measured, it was further hypothesized that the pH in the proximal endolymph is lower than the distal endolymph as increased otolith calcification would locally increase  $[H^+]$  (Payan et al., 1999). This heterogeneity of the proximal and distal endolymph was proposed to be the result of differential ion transporting activity of meshwork and patches ionocytes. Under this model, the larger NKA-rich ionocytes in the meshwork area remove  $K^+$  from the proximal endolymph, whereas the smaller NKA-rich ionocytes in the patches area secrete  $K^+$  and absorb  $H^+$  at the distal endolymph (Payan et al., 1999; Allemand et al., 2008). Similarly, other studies speculated that the larger meshwork CA-rich ionocytes remove  $H^+$  from the proximal endolymph (Tohse et al., 2006). These models imply that NKA-rich and CA-rich ionocytes in the meshwork area should express different proteins than their counterparts in the patches area.

Although many other proteins are known to be expressed in the fish inner ear, to our knowledge NKA and CA are the only two ion-transporting proteins established to be specifically present in ionocytes. Basolateral  $Na^+-K^+-2Cl^-$ -co-transporter (NKCC1; *slc12a2*), NKCC1 is expressed in their developing inner ear of Zebrafish (*Danio rerio*) larvae (Abbas and Whitfield, 2009). Although the lack of endolymph accumulation upon NKCC1 genetic disruption indicated a role in  $K^+$  and fluid secretion, the specific cell type where this protein is expressed was not established. Another study detected abundant intracellular acidic compartments in a subset of trout inner ear epithelial cells and hypothesized it indicated removal of  $H^+$  from the endolymph

by V-type H<sup>+</sup>-ATPase (VHA) (Mayer-Gostan et al., 1997). However, a subsequent study did not find VHA in Zebrafish inner ear ionocytes, and instead reported VHA expression within inner ear sensory hair cells and proposed it acidified the proximal endolymph to retard otolith calcification and maintain distance with the hair cells (Shiao et al., 2005). The plasma membrane Ca<sup>2+</sup>-ATPase (PMCA; *atp2b1a*) was proposed to be expressed in MR-ionocytes and to transport Ca<sup>2+</sup> for otolith calcification (Mugiya and Yoshida, 1995; Payan et al., 2002). *In situ* hybridization showed the presence of PMCA mRNA in some epithelial cells surrounding the sensory macula of the developing inner ear of Zebrafish larvae; however, attempts to immunolocalize the protein were unsuccessful in both larval and adult tissues and thus remain unknown whether PMCA is expressed in ionocytes (Cruz et al., 2009). More recently, a comprehensive transcriptomic and proteomic study concluded NKA, CA, VHA, and PMCA are expressed in the inner ear of black bream (*Acanthopagrus butcheri*) (Thomas et al., 2019). However, those analyses were conducted on samples that contained both inner ear and brain tissue, and thus did not provide insights about protein expression in specific cells. In summary, there are many excellent studies about the ion-transporting proteins involved in otolith calcification, but their use of different fish species, life stages, and techniques greatly complicates attempts to synthesize the available information into a single model describing the ion transporting mechanisms that maintain the distinctive endolymph composition necessary for proper inner ear function.

Although the cellular mechanisms underlying otolith calcification are not completely understood, it is clear that they activities are sensitive to acid-base conditions (reviewed in Allemand et al., 2008). Indeed, diurnal fluctuations in plasma [HCO<sub>3</sub><sup>-</sup>] is one of the underlying causes of the otolith's characteristic concentric rings (Tohse and Mugiya, 2008) used to estimate age and growth in stock assessment studies (Pannella, 1971; Campana and Neilson, 1985). And more recently, exposure to ocean acidification conditions has been reported to induce increased otolith size and density in multiple fish species (Checkley et al., 2009; Bignami et al., 2013; Maneja et al., 2013; Munday et al., 2011; Pimentel et al., 2014; Schade et al., 2014; Shen et al., 2016), which has been linked to plasma [HCO<sub>3</sub><sup>-</sup>] accumulation resulting from blood acid-base regulation [c.f. (Esbaugh et al., 2012, 2016)]. One possibility is that otolith overgrowth is the direct result of increased transport of plasma [HCO<sub>3</sub><sup>-</sup>] into the endolymph. However, increased otolith calcification rate also requires increased secretion of Ca<sup>2+</sup> and glycoprotein into the

endolymph, and increased H<sup>+</sup> removal. With this in mind, we explored whether the soluble adenylyl cyclase (sAC, adcy10) is expressed within inner ear epithelial ionocytes. This evolutionary conserved acid-base sensing enzyme is stimulated by HCO<sub>3</sub><sup>-</sup> to produce cyclic adenosine monophosphate (cAMP), a messenger molecule that can regulate multiple cellular processes *via* protein kinase A mediated phosphorylation on target proteins (reviewed in Tresguerres et al., 2010a; Tresguerres, 2014).

The goal of the current study was to determine how many types of ionocytes are present in the inner ear epithelium of a single species, the Pacific Chub Mackerel (*Scomber japonicus*, Houttuyn, 1782). To this end, we performed thorough immunohistochemical analyses using specific antibodies against NKA, CA, NKCC, VHA, PMCA, and sAC. Unexpectedly, we also detected high abundance of some of these proteins in the cells that form the arterioles that supply blood to the meshwork area. The resulting model about the ion-transporting and regulatory mechanisms underlying endolymph's unique composition improves our understanding about how otoliths are calcified, and will inform subsequent experimental studies to determine if and how they might be affected during environmental stress.

## **Methods:**

### *Tissue Sampling and Preparation*

Pacific Chub Mackerel were caught by hook and line off the Scripps pier in San Diego, United States (standard length =  $15.3 \pm 0.3$  cm; weight =  $26.9 \pm 2.2$  g; n = 19). In accordance to protocol S10320 of the University of California, San Diego Institutional of Animal Care and Use Committee, fish were euthanized by spinal pithing and its inner ear tissue dissected. Tissue was either flash frozen in liquid nitrogen and stored in -80°C, or fixed in 4% paraformaldehyde in phosphate buffer saline (PBS) at 4°C for 8 hours, incubated in 50% ethanol for 8 hours, and stored in 70% ethanol for immunohistochemistry. Protein integrity was prioritized; therefore, the length and weight of the fish were recorded after dissection.

### *Antibodies*

Mitochondria were labeled using a mouse monoclonal antibody against human cytochrome *c* oxidase complex IV (MTC02, catalog #: MA5-12017, Invitrogen, Grand Island, New York, USA); this antibody demonstrates specificity against a broad range of species

including coral (Barott et al., 2015b) and shark (Roa et al., 2014). The mouse monoclonal anti-NKA antibody  $\alpha 5$  (Lebovitz et al., 1989) was purchased from the Developmental Studies Hybridoma Bank (DSHB, The University of Iowa, Iowa City, IA, USA). This antibody has been extensively validated in fish and is routinely used to detect NKA in multiple fish tissues (Wilson et al., 2000, 2002; Roa et al., 2014; Roa and Tresguerres, 2017; Kwan et al., 2019). Additionally, NKA was immunodetected using rabbit polyclonal antibodies against the mammalian NKA  $\alpha$ -subunit (H300, catalog # SC-28800, Santa Cruz Biotechnology, Dallas, USA), which recognize NKA in gills from multiple fish (Roa et al., 2014; Michael et al., 2016; Allmon and Esbaugh, 2017). Rabbit polyclonal antibodies against human CA II were purchased from Rockland Inc., Gilbertsville, USA (catalog #: 100-401-136); these antibodies are routinely used to immunodetect CA from teleost fish [e.g. (Georgalis et al., 2006; Qin et al., 2010)], including in the saccular epithelium of Masu Salmon (*Oncorhynchus masou*) (Tohse et al., 2004). The mouse monoclonal anti-NKCC antibody T4 (Lytle et al., 1995) was obtained from DSHB; and has been widely used to detect NKCC in fish tissues (Tresguerres et al., 2010b; Esbaugh and Cutler, 2016), including Zebrafish saccular epithelium (Abbas and Whitfield, 2009). VHA was immunodetected using custom-made rabbit polyclonal antibodies against a peptide in the B subunit (epitope: AREEVPGRRGFPY; GenScript, Piscataway, USA); this peptide is conserved from cnidarians to mammals (Barott et al., 2015), and has been successfully used to immunodetect VHA in elasmobranch tissues (Roa et al., 2014; Roa and Tresguerres, 2017). The mouse monoclonal anti-PMCA antibody 5F10 against human erythrocyte PMCA was purchased from ThermoFisher Scientific, Waltham, USA (catalog #: MA3-914). sAC was immunodetected using custom-made rabbit polyclonal antibodies against a peptide in the first catalytic domain of Rainbow Trout sAC (epitope: LSSKKGYGADELTR; GenScript). The secondary antibodies were goat anti-mouse IgG-HRP and goat anti-rabbit IgG-HRP conjugate (Bio-Rad, Hercules, CA, USA) for western blot, and goat anti-mouse Alexa Fluor 546, goat anti-rabbit Alexa Fluor 488, and/or goat anti-rabbit Alexa Fluor 555 (Invitrogen, Grand Island, USA) for immunohistochemistry. Each antibody was tested in inner ear samples from at least three different fishes.

#### *Western Blotting*

Inner ear tissue was immersed in liquid nitrogen, pulverized in a porcelain grinder, and submerged in an ice-cold, protease inhibiting buffer (250 mmol l<sup>-1</sup> sucrose, 1 mmol l<sup>-1</sup> EDTA, 30 mmol l<sup>-1</sup> Tris, 10 mmol l<sup>-1</sup> benzamidine hydrochloride hydrate, 200 mmol l<sup>-1</sup> phenylmethanesulfonyl fluoride, 1 mol l<sup>-1</sup> dithiothreitol, pH 7.5). Next, debris was removed by low speed centrifugation (3000xg, 10 minutes, 4°C). Total protein concentration in the crude homogenate was determined by the Bradford assay (Bradford, 1976). Samples were mixed with an equal volume of 90% 2x Laemmli buffer and 10% β-mercaptoethanol, and heated at 70°C for 5 minutes. Protein (10 µg per lane) were loaded onto a 7.5% polyacrylamide mini gel (Bio-Rad, Hercules, CA, USA) and ran at 200 volts for 40 minutes, then transferred to a polyvinylidene difluoride (PVDF) membrane using a Trans-Blot SD Semi-Dry Transfer Cell (Bio-Rad). PVDF membranes were then incubated in tris-buffered saline with 1% tween (TBS-T) with milk powder (0.1 g/mL) at room temperature (RT) for 1 hour, then incubated with primary antibody (a5: 10.5 ng/ml; H300: 100 ng/ml; CA II antibody: 8 µg/ml; T4: 10.4 ng/ml; VHA *b*-subunit: 1.5 µg/ml; Rainbow Trout sAC: 3 µg/ml; 5F10: diluted 1:10,000 from commercial stock) in blocking buffer at 4°C overnight. On the following day, PVDF membranes were washed in TBS-T (three times; 10 minutes each), incubated in the appropriate anti-rabbit or anti-mouse secondary antibodies (1:10,000) at RT for 1 hour, and washed again in TBS-T (three times; 10 minutes each). Bands were made visible through addition of ECL Prime Western Blotting Detection Reagent (GE Healthcare, Waukesha, WI) and imaged and analyzed in a BioRad Universal III Hood using Image Lab software (version 6.0.1; BioRad). Peptide preabsorption with excess peptide (1:5 antibody to peptide ratio; preabsorbed overnight at 4°C on shaker) was performed to verify antibody specificity.

### *Immunostaining*

After fixation, samples were immersed in decalcifying solution (NaCl 450 mM, KCL 10 mM, MgCl 58 mM, Hepes 100 mM, EDTA 0.5 M, pH 7.5, changed daily) for three days at 4°C on a shake table to dissolve the otolith. Once the otolith dissolved, samples were incubated overnight in 70% ethanol and dehydrated through a series of increasing ethanol steps (70%, 95%, 100%, 10 minutes each), SafeClear (3 times; 10 minutes each), warm paraffin (65°C; 3 times; 10 minutes each), before embedding tissue in a paraffin block on an ice pack overnight. The next day, samples were sectioned using a microtome (~10 µm thickness) and mounted onto glass

slides. After drying overnight, paraffin was removed by incubation in SafeClear (3 times; 10 minutes each), and rehydrated in a series of decreasing ethanol steps (100%, 95%, 70%, 10 minutes each). To counter native autofluorescence, samples were immersed with sodium borohydride (1 mg/mL) in ice cold PBS (6 times; 10 minutes each). Samples were then washed in PBS + 0.1% tween (PBS-T) at RT for 5 minutes, incubated in blocking buffer (PBS-T, 0.02% normal goat serum, 0.0002% keyhole limpet hemocyanin) at RT for one hour, and with the primary antibodies (MTC02: 2 µg/ml; a5: 42 ng/ml; H300: 4 µg/ml; CA II antibody: 160 µg/ml; T4: 104 ng/ml; VHA *b*-subunit: 6 µg/ml; Rainbow Trout sAC: 6 µg/ml; 5F10: diluted 1:500 from commercial stock) in blocking buffer and kept in a humid chamber at RT overnight. On the following day, samples were washed in PBS-T (3 times; 10 minutes each) and incubated with the appropriate anti-rabbit or anti-mouse fluorescent secondary antibodies (1:1,000) and nuclear stain Hoechst 33342 (5 µg/mL; Invitrogen) at RT for 1 hour. Samples were washed in PBS-T (three times; 10 minutes each), then mounted in Fluoro-gel with Tris (Electron Microscopy Sciences). Samples were examined and imaged on an epifluorescence microscope (Zeiss AxioObserver Z1). Digital images were adjusted, for brightness and contrast, using Zeiss Axiovision software. Some low magnification images were stitched together to provide pictures of the entire saccular epithelium using Helicon Focus 6 (Helicon Soft Ltd., Kharkov, Ukraine). Peptide preabsorption with excess peptide (1:10 antibody to peptide ratio; preabsorbed overnight at 4°C on shaker) was performed to verify antibody specificity against VHA and sAC.

## Results:

Western blotting revealed high abundance of NKA, CA, NKCC, VHA, sAC, and PMCA protein in Pacific Chub Mackerel inner ears (Fig. 1). The immunoreactive bands matched the predicted size of each target protein (NKA- $\alpha$  subunit: ~100 kDa with both mono- and polyclonal antibodies; CA: ~30 kDa; NKCC: ~200 kDa; VHA-*b* subunit: ~55 kDa; PMCA: ~140 kDa; sAC: ~180, 110, and 50 kDa), were sharp and distinct, and were absent in control blots in which the primary antibody was omitted. No bands were detected in anti-VHA and anti-sAC antibodies' pre-immune and peptide pre-absorption controls.

Next, we examined the expression of these proteins within specific saccular epithelial cells using immunohistochemistry. NKA was abundantly expressed within cells adjacent to the endolymph (Fig. 2a). Higher magnification images revealed NKA immunostaining produced a



dense intracellular speckled pattern (Fig. 2b), which indicates NKA is present in the highly infolded basolateral membrane. Double immunolabeling with anti-complex IV antibodies revealed the NKA-rich ionocytes are MR (Fig. 2c) and contain abundant NKCC (Fig. 2d). Furthermore, the resulting “yellow” signal from dual NKA and NKCC immunolabeling indicated a strong overlap in the basolateral membrane. CA was also highly expressed in specific saccular epithelial cells; however, double immunolabeling revealed CA was present in cells that were not labeled for NKA (Fig. 3a) or NKCC1 (Fig. 3b). Similarly, double immunolabeling of NKA and VHA (Fig. 4a, b, c) revealed that these two proteins were expressed in different cells. By default, this indicates the CA and VHA were expressed in the same cell type. Overall, these results indicate the presence of two types of ionocytes in the saccular epithelium. “Type-I” ionocytes abundantly express NKA and NKCC1 and are MR, and “Type-II” ionocytes abundantly express CA and VHA.

PMCA was also abundantly expressed in saccular epithelial cells adjacent to the endolymph. The pattern observed following dual immunostaining with NKA indicates PMCA is present in Type-I and Type-II ionocytes (Fig. 5a, b). Unlike NKA and NKCC1 (Fig. 2d), NKA and PMCA immunofluorescent signals did not overlap significantly (Fig. 5c), suggesting PMCA is predominantly present in cytoplasmic vesicles and not in the basolateral membrane.

Additionally, abundant sAC immunolabeling was detected throughout the saccular epithelium (Fig. 5d). Dual immunostaining of sAC and NKA (Fig. 5e, f) and sAC and PMCA (Fig. 5g, h, i) revealed sAC was abundantly expressed in both Type-I and Type-II ionocytes.

Type-I and Type-II ionocytes in the meshwork area were larger than in the patches area (~40  $\mu\text{m}$  vs. ~10  $\mu\text{m}$  wide, respectively; Fig. 4b, c). However, the protein expression profile in each ionocyte type was identical regardless of size. In addition to the previously reported presence of PMCA (Cruz et al., 2009) and VHA (Shiao et al., 2005), we detected NKA (Fig. 2a) and sAC (Fig. 5d) within the sensory hair cells. Unexpectedly, we also observed intense CA (Fig. 6a, b), VHA (Fig. 6c, d), and sAC (Fig. 6e, f) immunoreactivity within the endothelial cells that form the abundant capillaries surrounding the meshwork area.

## **Discussion:**

Here, we characterized two types of ionocytes within the Pacific Chub Mackerel's saccular epithelium: Type-I ionocytes are MR and express abundant NKA, NKCC1, PMCA, and

sAC whereas Type-II ionocytes express abundant CA, VHA, PMCA, and sAC (Fig. 8). Ionocyte distribution and size patterns were similar to those reported in most previous studies (Mayer-Gostan et al., 1997; Pisam et al., 1998): larger ionocytes bordered the meshwork area while smaller ionocytes were found in the patches area. However, there were no differences in protein expression between the larger Type-I and Type-II meshwork ionocytes and the smaller Type-I and Type-II patches ionocytes, further supporting the idea that only two types of ionocytes exist within the saccular epithelium. This suggests that the differences in ionic composition between the proximal and distal endolymph are the result of different ion transporting rates in these two regions and not due to the presence of different ion transporting mechanisms. Additional factors that surely contribute to the heterogeneous endolymph ionic composition and otolith calcification rates include the activity of hair cells and the secretion of glycoproteins that promote carbonate precipitation, both taking place in the meshwork area and proximal endolymph (reviewed in Payan et al., 2004; Allemand et al., 2008).

Our results on the marine Pacific Chub Mackerel generally agree with the literature about ion transporting mechanisms in fish inner ear epithelia, which is largely based on research on freshwater fishes. The main differences were the localization of VHA and PMCA. The former was reported to be exclusively expressed in sensory hair cells in the inner ear of Zebrafish embryos (Shiao et al., 2005), and the latter was only studied at the mRNA level and predominantly found in hair cells as well (Cruz et al., 2009). Future experiments should confirm whether the differences between Pacific Chub Mackerel and Zebrafish are species or life stage-specific, environmentally based (i.e. freshwater vs seawater), or due to different immunostaining techniques and antibodies.

#### *Putative functions of fish inner ear epithelial ionocyte function.*

Based on the presence of NKA and NKCC1, the Type-I ionocytes are likely responsible for secreting  $K^+$  into the endolymph, where it can reach concentrations  $>40$  higher than in blood plasma (Payan et al., 1997, 1999; Ghanem et al., 2008). Given that NKCC1 knockout results in inner ear collapses due to lack of fluid in Zebrafish larvae (Abbas and Whitfield, 2009), one of the roles of NKCC1-driven  $K^+$  secretion is to osmotically drive fluid transport. Additionally, the  $K^+$ -rich endolymph is essential for mechanoreception by the sensory hair cells (Zdebik et al., 2009). This model would imply that Type-I ionocytes express  $K^+$  channels in their apical

membrane, and should be further investigated in future studies. The outwardly conducting KCNQ1/KCNE1 K<sup>+</sup> channels found on the apical membrane of the analogous “dark” cells of mammalian inner ear are promising candidates (Nicolas et al., 2001).

In contrast, the high abundance of CA and VHA in Type-II ionocytes suggests these cells are involved in promoting otolith calcification by secreting HCO<sub>3</sub><sup>-</sup> into the endolymph and removing H<sup>+</sup>. The CA-catalyzed hydration of CO<sub>2</sub> (for example from the abundant mitochondria from the adjacent Type-I ionocytes) would provide HCO<sub>3</sub><sup>-</sup> to be secreted into the endolymph by yet unidentified apical anion exchangers. The H<sup>+</sup> that is simultaneously produced might be removed by VHA, either into intracellular vesicles as proposed by Mayer-Gostan *et al* (1997) or upon VHA insertion into the basolateral membrane as reported in the base-secreting cells of elasmobranch gills (Tresguerres et al., 2005; Roa and Tresguerres, 2016).

Both Type-I and Type-II ionocytes also expressed PMCA, which has been previously shown to be important for otolith calcification based on the effects of genetic knockdown (Cruz et al., 2009) and pharmacological inhibition of calmodulin-antagonist of PMCA activity (Mugiya and Yoshida, 1995). The presence of PMCA throughout the cytoplasm suggests Ca<sub>2</sub><sup>+</sup> sequestration in vesicles, which may be transported to the apical membrane and its contents exocytosed into the calcifying fluid as proposed in coral calcifying cells (Barott et al., 2015b; Barron et al., 2018). Other proposed transcellular pathways for Ca<sub>2</sub><sup>+</sup> transport include Ca<sub>2</sub><sup>+</sup> channels and Na<sup>+</sup>/Ca<sub>2</sub><sup>+</sup> exchangers (Mugiya and Yoshida, 1995; Thomas et al., 2019), and the identification of their cellular and subcellular localizations would contribute greatly to the mechanistic model of otolith calcification.

#### *A potential regulatory mechanism of otolith calcification.*

Both Type-I and Type-II ionocytes contained sAC, an evolutionary conserved acid-base sensing enzyme that produces the messenger molecule cAMP (Chen et al., 2000; Tresguerres, 2014). The effects of plasma and endolymph acid-base status on otolith calcification are well established (Takagi, 2002; Payan et al., 2004; Allemand et al., 2008), and sAC may be one of the underlying signaling mechanisms that senses and regulates the activity of calcification-relevant ion transporting proteins. Supporting this possibility, some of the same ion-transporting proteins found in Type-I and Type-II ionocytes have been shown to be under sAC regulation in many other epithelia. In the intestine of marine teleosts, sAC senses elevations in [HCO<sub>3</sub><sup>-</sup>] and

regulates NKA and NKCC activity to promote luminal carbonate precipitation and fluid transport (Tresguerres et al., 2010b; Carvalho et al., 2012). In marine elasmobranchs gills, sAC senses blood alkalosis and activates VHA -and possibly the apical anion exchanger pendrin- to mediate compensatory  $\text{HCO}_3^-$  secretion and  $\text{H}^+$  absorption (Tresguerres et al., 2010c; Roa et al., 2014; Roa and Tresguerres, 2016). In addition to being directly stimulated by  $\text{HCO}_3^-$ , sAC is stimulated by  $\text{Ca}^{2+}$  (Litvin et al., 2003), providing another potential regulatory mechanism for otolith calcification. Interestingly, sAC is also abundantly expressed in coral calcifying cells (Barott et al., 2017) and in oyster mantle (Barron et al., 2012), suggesting a conserved role in regulating transepithelial ion transport for calcification.

#### *A novel regulatory role of capillaries in regulating otolith calcification?*

The connective tissues surrounding the inner ear contain numerous capillaries, which are especially abundant near the meshwork area (Saitoh, 1990; Mayer-Gostan et al., 1997). Unexpectedly, we found the endothelial cells that form such capillaries to abundantly express CA, VHA, and sAC. This is consistent with previous reports of CA within the cytoplasm of capillaries in the analogous mammalian inner ear (Watanabe and Ogawa, 1984). We tentatively propose that the activities of these proteins are relevant for otolith calcification by mediating the transport of  $\text{CO}_2/\text{HCO}_3^-$  from the blood to the endolymph, and by facilitating the removal of excess  $\text{H}^+$  generated as a result of  $\text{CaCO}_3$  precipitation. In addition, the local acidification of the capillary lumen could trigger the Root effect in circulating red blood cells, thus promoting  $\text{O}_2$  offloading to sustain aerobic metabolism of ionocytes and sensory hair cells within the saccular epithelium. Such a mechanism was originally described in fish swim bladder and eye (reviewed in Pelster, 2001), and more recently proposed to apply more broadly to other highly aerobic fish tissues including the eye (Fairbanks et al., 1969), muscle (Rummer et al., 2013), and intestine (Cooper et al., 2014).

#### *Conclusions, future directions and significance.*

Our proposed model is consistent with previous functional studies conducted on isolated fish inner ear organ that suggested the involvement of NKA, CA, and PMCA (as well as  $\text{Na}^+/\text{Ca}^{2+}$  exchanger,  $\text{Ca}^{2+}$  channels, and  $\text{Na}^+/\text{H}^+$  exchanger) based on acid-base titration and  $^{45}\text{Ca}^{2+}$  incorporation experiments in combination with pharmacological inhibitors (Mugiya and

Yoshida, 1995; Payan et al., 1997). Furthermore, functional evidence for the roles of NKCC1 (Abbas and Whitfield, 2009) and PMCA (Cruz et al., 2009) is available through the genetic downregulation experiments on Zebrafish larvae mentioned above. More recently, the presence of many of those proteins as well as VHA has been confirmed through an extensive proteomic and transcriptomic survey (Thomas et al., 2019) (with the caveat that analyses were conducted on samples that contain both inner ear and brain tissue). Our results expand and complement those previous studies by establishing the transporter's cellular and subcellular localization, ultimately leading to the identification of two types of ionocytes. In addition, our results revealed sAC is present in both types of ionocytes, providing a potential mechanism that can regulate otolith calcification in response to acid-base variations. Ongoing efforts in our laboratory are attempting to functionally characterize the putative regulatory role of sAC on inner ear function; however, sAC's presence within both types of ionocytes, sensory hair cells, and capillaries is a significant hurdle for studies at the organ and whole organism level. For example, putative changes in protein or mRNA abundance in ionocytes in response to experimental manipulations would be confounded by the background provided by all the other cell types in the tissue, which are the majority. Thus, detailed functional studies on the underlying ion transport mechanism would require the development of ionocyte primary cultures. Similar considerations apply to efforts to elucidating the functional roles of CA, VHA, and sAC in the capillaries near the meshwork area.

The inner ear organ allows fish to sense and respond to its environment and therefore is essential for survival. In addition, analyses on otolith rings provide valuable information regarding daily and seasonal growth bands, trace element signatures (Swearer et al., 1999), exposure to environmental salinity and temperature (Campana, 1999; Elsdon and Gillanders, 2002), and diet (Radtke et al., 1996; Nelson et al., 2011; von Biela et al., 2015). Thus, in addition to its intrinsic value from physiological and evolutionary perspectives, information about the cellular mechanisms underlying otolith calcification can improve current fisheries assessment tools and help predict the effects of environmental stressors, and in particular ocean acidification, on otolith growth and function from a mechanistic perspective.

#### **Acknowledgements:**

GTK was supported by the National Science Foundation (NSF) Graduate Research

Fellowship Program and the NSF Graduate Research Internship Program. This research was supported by grant NSF IOS #1754994 to M.T. We thank Jake Munich for his assistance in capturing Pacific Chub Mackerel.

### Figure Captions:

Fig. 1: Western blot analysis of inner ear homogenates. Antibodies against monoclonal Na<sup>+</sup>/K<sup>+</sup>-ATPase (mNKA), polyclonal Na<sup>+</sup>/K<sup>+</sup>-ATPase (pNKA), carbonic anhydrase (CA), Na<sup>+</sup>-K<sup>+</sup>-Cl<sup>-</sup>-co-transporter (NKCC), V-type H<sup>+</sup> ATPase (VHA), plasma membrane calcium ATPase (PMCA), and soluble adenylyl cyclase (sAC) reveal bands matching the predicted size of respective proteins. Molecular marker is shown on the left of each respective blot.

Fig. 2: Characterization of Type-I ionocytes within the saccular epithelium. Histological saggital section immunostained with (a) Na<sup>+</sup>/K<sup>+</sup>-ATPase (NKA, green). (b) Magnified view of the NKA-rich ionocytes revealed abundant staining in a dense, speckled pattern resembling a developed basolateral infolding. Dual-immunostaining revealed the NKA-rich (green) ionocyte is also (c) mitochondrion-rich (red) and contain abundant (d) Na<sup>+</sup>-K<sup>+</sup>-2Cl<sup>-</sup>-co-transporter (NKCC, red). Nuclei are stained blue. EN = endolymph. SO = saggital otolith protein. SHC = sensory hair cell.

Fig. 3: Evidence for two types of ionocytes within the saccular epithelium. Dual-immunostaining of ionocytes within the saccular epithelium revealed carbonic anhydrase (CA; red) is expressed in cells that are different from the (a) Na<sup>+</sup>/K<sup>+</sup>-ATPase (NKA; green) and (b) Na<sup>+</sup>-K<sup>+</sup>-2Cl<sup>-</sup>-co-transporter (NKCC, green)-rich Type-I ionocyte. Nuclei are stained blue. EN = endolymph.

Fig. 4: Characterization of Type-II ionocytes within the saccular epithelium. (a) Histological saggital section immunostained with Na<sup>+</sup>/K<sup>+</sup>-ATPase (NKA, green) and V-type H<sup>+</sup>-ATPase (VHA, red). (b) Higher magnification image of saccular ionocytes of the larger meshwork ionocytes and (c) the smaller patches ionocytes indicate NKA-rich and VHA-rich cells are different cells. Nuclei are stained blue. EN = endolymph; SO = saggital otolith protein. SHC = sensory hair cell.

Fig. 5: Presence of plasma membrane  $\text{Ca}^{2+}$  ATPase and soluble adenylyl cyclase in Type-I and Type-II ionocytes. (a, b, c) Dual immunostaining of plasma membrane  $\text{Ca}^{2+}$ -ATPase (PMCA, green) with  $\text{Na}^{+}/\text{K}^{+}$ -ATPase (NKA, red). Notice that PMCA is present in all NKA-rich cells (Type-I ionocyte), as well as in adjacent cells without NKA signal (Type-II ionocytes). (d) Histological sagittal section immunostained with soluble adenylyl cyclase (sAC, red) and  $\text{Na}^{+}/\text{K}^{+}$ -ATPase (NKA, green). (e,f) higher magnification images reveal sAC is present in both the NKA-rich Type-I ionocytes (green) and Type-II ionocytes (indicated by ionocytes lacking NKA signal). (g, h, i) The presence of PMCA (green) and sAC (red) in both Type-I and Type-II ionocytes was further conformed by dual-staining. Nuclei are stained blue. EN = endolymph; SO = sagittal otolith protein. SHC = sensory hair cell.

Fig. 6: Inner ear saccular epithelium capillaries express CA, VHA, and sAC. Histological section dual-stained with (a, b) carbonic anhydrase (CA, red) and  $\text{Na}^{+}-\text{K}^{+}-2\text{Cl}^{-}$ -co-transporter (NKCC, green), (c, d) V-type  $\text{H}^{+}$ -ATPase-rich (VHA, green) and  $\text{Na}^{+}/\text{K}^{+}$ -ATPase (NKA, green), and (e, f) soluble adenylyl cyclase (sAC, red) and NKA (green). Nuclei are stained blue. EN = endolymph; CAP = capillary.

Fig. 7: Proposed model for otolith calcification by the two types of ionocytes within the inner ear saccular epithelium. Abbreviations:  $\text{Na}^{+}/\text{K}^{+}$ -ATPase (NKA),  $\text{Na}^{+}-\text{K}^{+}-\text{Cl}^{-}$ -co-transporter (NKCC), mitochondria (mito), carbonic anhydrase (CA), V-type  $\text{H}^{+}$  ATPase (VHA), plasma membrane calcium ATPase (PMCA), soluble adenylyl cyclase (sAC), anion exchanger (AE), and  $\text{K}^{+}$  channel (KC). Capillaries that supply  $\text{O}_2$  (and potentially  $\text{HCO}_3^{-}$ ) are not shown for simplicity, though they are especially important in the meshwork area. Ion transport is indicated by a solid line, and gas diffusion is indicated by a dashed, squiggly line.

## Reference:

- Abbas L, Whitfield TT (2009) *Nkcc1* (*Slc12a2*) is required for the regulation of endolymph volume in the otic vesicle and swim bladder volume in the zebrafish larva. *Development* 136:2837–2848. doi: 10.1242/dev.034215
- Allemand D, Mayer-Gostan N, De Pontual H, Boeuf G, Payan P (2008) Fish otolith calcification in relation to endolymph chemistry. *Handb Biominer Biol Asp Struct Form* 1:291–308. doi: 10.1002/9783527619443.ch17

465 Allmon EB, Esbaugh AJ (2017) Carbon dioxide induced plasticity of branchial acid-base  
466 pathways in an estuarine teleost. *Sci Rep* 7:45680. doi: 10.1038/srep45680

467 Barott K, Venn AA, Perez SO, Tambutté S, Tresguerres M (2015a) Coral host cells acidify  
468 symbiotic algal microenvironment to promote photosynthesis. *Proc Natl Acad Sci U S A*  
469 112:607–12. doi: 10.1073/pnas.1413483112

470 Barott KL, Perez SO, Linsmayer LB, Tresguerres M (2015b) Differential localization of ion  
471 transporters suggests distinct cellular mechanisms for calcification and photosynthesis  
472 between two coral species. *Am J Physiol - Regul Integr Comp Physiol* 309:R235–R246. doi:  
473 10.1152/ajpregu.00052.2015

474 Barott KL, Barron ME, Tresguerres M (2017) Identification of a molecular pH sensor in coral.  
475 *Proc R Soc B Biol Sci* 284:20171769. doi: 10.1098/rspb.2017.1769

476 Barron ME, Roa JNBR, Tresguerres M (2012) Pacific oyster mantle, gill and hemocytes express  
477 the bicarbonate-sensing enzyme soluble adenylyl cyclase. In: *FASEB journal : official*  
478 *publication of the Federation of American Societies for Experimental Biology.*

479 Barron ME, Thies AB, Espinoza JA, Barott KL, Hamdoun A, Tresguerres M (2018) A vesicular  
480 Na<sup>+</sup>/Ca<sup>2+</sup> exchanger in coral calcifying cells. *PLoS One* 13:e0205367. doi:  
481 10.1371/journal.pone.0205367

482 Beier M, Anken R, Hilbig R (2006) Sites of calcium uptake of fish otoliths correspond with  
483 macular regions rich of carbonic anhydrase. *Adv Sp Res* 38:1123–1127. doi:  
484 10.1016/j.asr.2005.10.042

485 Bignami S, Enochs IC, Manzello DP, Sponaugle S, Cowen RK (2013) Ocean acidification alters  
486 the otoliths of a pantropical fish species with implications for sensory function. *Proc Natl*  
487 *Acad Sci* 110:7366–7370. doi: 10.1073/pnas.1301365110

488 Borelli G, Guibbolini ME, Mayer-Gostan N, Priouzeau F, De Pontual H, Allemand D, et al  
489 (2003) Daily variations of endolymph composition: relationship with the otolith calcification  
490 process in trout. *J Exp Biol* 206:2685–2692. doi: 10.1242/jeb.00479

491 Bradford MM (1976) A rapid and sensitive method for the quantitation of microgram quantities  
492 of protein utilizing the principle of protein-dye binding. *Anal Biochem* 72:248–254. doi:  
493 10.1016/0003-2697(76)90527-3

494 Campana S (1999) Chemistry and composition of fish otoliths: pathways, mechanisms and  
495 applications. *Mar Ecol Prog Ser* 188:263–297. doi: 10.3354/meps188263

496 Campana SE, Neilson JD (1985) Microstructure of fish otoliths. *Can J Fish Aquat Sci* 42:1014–  
497 1032.

498 Carvalho ESM, Gregório SF, Power DM, Canário AVM, Fuentes J (2012) Water absorption and  
499 bicarbonate secretion in the intestine of the sea bream are regulated by transmembrane and  
500 soluble adenylyl cyclase stimulation. *J Comp Physiol B Biochem Syst Environ Physiol*  
501 182:1069–1080. doi: 10.1007/s00360-012-0685-4



502 Checkley DM, Dickson AG, Takahashi M, Radich JA, Eisenkolb N, Asch R (2009) Elevated  
503 CO<sub>2</sub> enhances otolith growth in young fish. *Science* 324:1683. doi: 10.1126/science.1169806

504 Chen Y, Cann MJ, Litvin TN, Iourgenko V, Sinclair ML, Levin LR, et al (2000) Soluble  
505 adenylyl cyclase as an evolutionarily conserved bicarbonate sensor. *Science* 289:625–8. doi:  
506 10.1126/science.289.5479.625

507 Cooper CA, Regan MD, Brauner CJ, De Bastos ESR, Wilson RW (2014) Osmoregulatory  
508 bicarbonate secretion exploits H<sup>+</sup>-sensitive haemoglobins to autoregulate intestinal O<sub>2</sub>  
509 delivery in euryhaline teleosts. *J Comp Physiol B Biochem Syst Environ Physiol* 184:865–  
510 876. doi: 10.1007/s00360-014-0844-x

511 Cruz S, Shiao JC, Liao BK, Huang CJ, Hwang PP (2009) Plasma membrane calcium ATPase  
512 required for semicircular canal formation and otolith growth in the zebrafish inner ear. *J Exp*  
513 *Biol* 212:639–647. doi: 10.1242/jeb.022798

514 Dijkgraaf S (1960) Hearing in bony fishes. *Proc R Soc B-Biological Sci* 152:51–54.

515 Elsdon TS, Gillanders BM (2002) Interactive effects of temperature and salinity on otolith  
516 chemistry: challenges for determining environmental histories of fish. *Can J Fish Aquat Sci*  
517 59:1796–1808. doi: 10.1139/f02-154

518 Esbaugh AJ, Heuer R, Grosell M (2012) Impacts of ocean acidification on respiratory gas  
519 exchange and acid-base balance in a marine teleost, *Opsanus beta*. *J Comp Physiol B*  
520 *Biochem Syst Environ Physiol* 182:921–934. doi: 10.1007/s00360-012-0668-5

521 Esbaugh AJ, Cutler B (2016) Intestinal Na<sup>+</sup>, K<sup>+</sup>, 2Cl<sup>-</sup>-cotransporter 2 plays a crucial role in  
522 hyperosmotic transitions of a euryhaline teleost. *Physiol Rep* 4:1–12. doi:  
523 10.14814/phy2.13028

524 Esbaugh AJ, Ern R, Nordi WM, Johnson AS (2016) Respiratory plasticity is insufficient to  
525 alleviate blood acid–base disturbances after acclimation to ocean acidification in the  
526 estuarine red drum, *Sciaenops ocellatus*. *J Comp Physiol B Biochem Syst Environ Physiol*  
527 186:97–109. doi: 10.1007/s00360-015-0940-6

528 Fairbanks MB, Hoffert JR, Fromm PO (1969) The dependence of the oxygen-concentrating  
529 mechanism of the teleost eye (*Salmo gairdneri*) on the enzyme carbonic anhydrase. *J Gen*  
530 *Physiol* 54:203–211. doi: 10.1085/jgp.54.2.203

531 Furukawa T, Ishii Y (1967) Neurophysiological studies on hearing in goldfish. *J Neurophysiol*  
532 30:1377–1403.

533 Georgalis T, Gilmour KM, Yorston J, Perry SF (2006) Roles of cytosolic and membrane-bound  
534 carbonic anhydrase in renal control of acid-base balance in rainbow trout, *Oncorhynchus*  
535 *mykiss*. *Am J Physiol - Ren Physiol* 291:407–421. doi: 10.1152/ajprenal.00328.2005

536 Ghanem TA, Breneman KD, Rabbitt RD, Brown HM (2008) Ionic composition of endolymph  
537 and perilymph in the inner ear of the oyster toadfish, *Opsanus tau*. *Biol Bull* 214:83–90. doi:  
538 10.2307/25066662

539 Ibsch M, Anken R, Beier M, Rahmann H (2004) Endolymphatic calcium supply for fish otolith  
540 growth takes place via the proximal portion of the otocyst. *Cell Tissue Res* 317:333–336. doi:  
541 10.1007/s00441-004-0930-6

542 Kwan GT, Wexler JB, Wegner NC, Tresguerres M (2019) Ontogenetic changes in cutaneous and  
543 branchial ionocytes and morphology in yellowfin tuna (*Thunnus albacares*) larvae. *J Comp*  
544 *Physiol B Biochem Syst Environ Physiol* 189:81–95. doi: 10.1007/s00360-018-1187-9

545 Ladich F, Schulz-Mirbach T (2016) Diversity in fish auditory systems: one of the riddles of  
546 sensory biology. *Front Ecol Evol* 4:1–26. doi: 10.3389/fevo.2016.00028

547 Lebovitz RM, Takeyasu K, Fambrough DM (1989) Molecular characterization and expression of  
548 the (Na<sup>+</sup> + K<sup>+</sup>)-ATPase alpha-subunit in *Drosophila melanogaster*. *EMBO J* 8:193–202.

549 Litvin TN, Kamenetsky M, Zarifyan A, Buck J, Levin LR (2003) Kinetic properties of “soluble”  
550 adenylyl cyclase: Synergism between calcium and bicarbonate. *J Biol Chem* 278:15922–  
551 15926. doi: 10.1074/jbc.M212475200

552 Lytle C, Xu JC, Biemesderfer D, Forbush B (1995) Distribution and diversity of Na-K-Cl  
553 cotransport proteins: a study with monoclonal antibodies. *Am J Physiol* 269:C1496–C1505.

554 Maneja RH, Frommel a. Y, Geffen a. J, Folkvord a., Piatkowski U, Chang MY, et al (2013)  
555 Effects of ocean acidification on the calcification of otoliths of larval Atlantic cod *Gadus*  
556 *morhua*. *Mar Ecol Prog Ser* 477:251–258. doi: 10.3354/meps10146

557 Mayer-Gostan N, Kossmann H, Watrin A, Payan P, Boeuf G (1997) Distribution of ionocytes in  
558 the saccular epithelium of the inner ear of two teleosts (*Oncorhynchus mykiss* and  
559 *Scophthalmus maximus*). *Cell Tissue Res* 289:53–61. doi: 10.1007/s004410050851

560 Michael K, Kreiss CM, Hu MY, Koschnick N, Bickmeyer U, Dupont S, et al (2016)  
561 Adjustments of molecular key components of branchial ion and pH regulation in Atlantic cod  
562 (*Gadus morhua*) in response to ocean acidification and warming. *Comp Biochem Physiol*  
563 *Part - B Biochem Mol Biol* 193:33–46. doi: 10.1016/j.cbpb.2015.12.006

564 Mugiya Y, Yoshida M (1995) Effects of Calcium Antagonists and Other Metabolic on in Vitro  
565 Calcium Deposition on Otoliths Rainbow Trout *Oncorhynchus mykiss* Modulators in the.  
566 *Fish* 61:1026–1030.

567 Munday PL, Hernaman V, Dixson DL, Thorrold SR (2011) Effect of ocean acidification on  
568 otolith development in larvae of a tropical marine fish. *Biogeosciences* 8:1631–1641. doi:  
569 10.5194/bg-8-1631-2011

570 Murayama E, Takagi Y, Ohira T, Davis JG, Greene MI, Nagasawa H (2002) Fish otolith  
571 contains a unique structural protein, otolin-1. *Eur J Biochem* 269:688–696. doi:  
572 10.1046/j.0014-2956.2001.02701.x

573 Nelson J, Hanson CW, Koenig C, Chanton J (2011) Influence of diet on stable carbon isotope  
574 composition in otoliths of juvenile red drum *Sciaenops ocellatus*. *Aquat Biol* 13:89–95. doi:  
575 10.3354/ab00354

576 Nicolas M-T, Demêmes D, Martin A, Kupersmidt S, Barhanin J (2001) KCNQ1/KCNE1  
577 potassium channels in mammalian vestibular dark cells. *Hear Res* 153:132–145. doi:  
578 10.1016/S0378-5955(00)00268-9

579 Pannella G (1971) Fish Otoliths : Daily Growth Layers and Periodical Patterns. *Science* (80- )  
580 173:1124–1127.

581 Payan P, Kossmann H, Watrin a, Mayer-Gostan N, Boeuf G (1997) Ionic composition of  
582 endolymph in teleosts: origin and importance of endolymph alkalinity. *J Exp Biol* 200:1905–  
583 1912.

584 Payan P, Edeyer A, de Pontual H, Borelli G, Boeuf G, Mayer-Gostan N (1999) Chemical  
585 composition of saccular endolymph and otolith in fish inner ear: lack of spatial uniformity.  
586 *Am J Physiol* 277:R123–R131.

587 Payan P, Borelli G, Priouzeau F, De Pontual H, Boeuf G, Mayer-Gostan N (2002) Otolith growth  
588 in trout *Oncorhynchus mykiss*: supply of Ca<sup>2+</sup> and Sr<sup>2+</sup> to the saccular endolymph. *J Exp*  
589 *Biol* 205:2687–2695. doi: Unsp Jeb4023

590 Payan P, De Pontual H, Bœuf G, Mayer-Gostan N (2004) Endolymph chemistry and otolith  
591 growth in fish. *Comptes Rendus Palevol* 3:535–547. doi: 10.1016/j.crpv.2004.07.013

592 Pelster B (2001) The Generation of Hyperbaric Oxygen Tensions in Fish. *Physiology* 16:287–  
593 291. doi: 10.1152/physiologyonline.2001.16.6.287

594 Pimentel MS, Faleiro F, Dionisio G, Repolho T, Pousao-Ferreira P, Machado J, et al (2014)  
595 Defective skeletogenesis and oversized otoliths in fish early stages in a changing ocean. *J*  
596 *Exp Biol* 217:2062–2070. doi: 10.1242/jeb.092635

597 Pisam M, Payan P, LeMoal C, Edeyer A, Boeuf G, Mayer-Gostan N (1998) Ultrastructural study  
598 of the saccular epithelium of the inner ear of two teleosts, *Oncorhynchus mykiss* and *Psetta*  
599 *maxima*. *Cell Tissue Res* 294:261–270. doi: 10.1007/s004410051176

600 Qin Z, Lewis JE, Perry SF (2010) Zebrafish (*Danio rerio*) gill neuroepithelial cells are sensitive  
601 chemoreceptors for environmental CO<sub>2</sub>. *J Physiol* 588:861–872. doi:  
602 10.1113/jphysiol.2009.184739

603 Radtke RL, Lenz P, Showers W, Moksness E (1996) Environmental information stored in  
604 otoliths: insights from stable isotopes. *Mar Biol* 127:161–170. doi: 10.1007/BF00993656

605 Roa JN, Munévar CL, Tresguerres M (2014) Feeding induces translocation of vacuolar proton  
606 ATPase and pendrin to the membrane of leopard shark (*Triakis semifasciata*) mitochondrion-  
607 rich gill cells. *Comp Biochem Physiol -Part A Mol Integr Physiol* 174:29–37. doi:  
608 10.1016/j.cbpa.2014.04.003

609 Roa JN, Tresguerres M (2016) Soluble adenylyl cyclase is an acid-base sensor in epithelial base-  
610 secreting cells. *Am J Physiol - Cell Physiol* 311:C340–C349. doi:  
611 10.1152/ajpcell.00089.2016

612 Roa JN, Tresguerres M (2017) Bicarbonate-sensing soluble adenylyl cyclase is present in the cell  
613 cytoplasm and nucleus of multiple shark tissues. *Physiol Rep* 5:e13090. doi:  
614 10.14814/phy2.13090

615 Rummer JL, McKenzie DJ, Innocenti A, Supuran CT, Brauner CJ (2013) Root Effect  
616 Hemoglobin May Have Evolved to Enhance General Tissue Oxygen Delivery. *Science*  
617 340:1327–1329. doi: 10.1126/science.1233692

618 Saitoh S (1990) Localization and ultrastructure of mitochondria-rich cells in the inner ears of  
619 goldfish and tilapia. *J Ichthyology* 37:49–55.

620 Schade FM, Clemmesen C, Mathias Wegner K (2014) Within- and transgenerational effects of  
621 ocean acidification on life history of marine three-spined stickleback (*Gasterosteus*  
622 *aculeatus*). *Mar Biol* 161:1667–1676. doi: 10.1007/s00227-014-2450-6

623 Shen SG, Chen F, Schoppik DE, Checkley DM (2016) Otolith size and the vestibulo-ocular  
624 reflex of larvae of white seabass *Atractoscion nobilis* at high pCO<sub>2</sub>. *Mar Ecol Prog Ser*  
625 553:173–182. doi: 10.3354/meps11791

626 Shiao JC, Lin LY, Horng JL, Hwang PP, Kaneko T (2005) How can teleostean inner ear hair  
627 cells maintain the proper association with the accreting otolith? *J Comp Neurol* 488:331–341.  
628 doi: 10.1002/cne.20578

629 Swearer SE, Caselle JE, Lea DW, Warner RR (1999) Larval retention and recruitment in an  
630 island population of a coral-reef fish. *Nature* 402:799–802. doi: 10.1038/45533

631 Takagi Y (1997) Meshwork arrangement of mitochondria-rich, Na<sup>+</sup>,K<sup>+</sup>-ATPase-rich cells in the  
632 saccular epithelium of rainbow trout (*Oncorhynchus mykiss*) inner ear. *Anat Rec* 248:483–  
633 489. doi: 10.1002/(SICI)1097-0185(199708)248:4<483::AID-AR1>3.0.CO;2-N

634 Takagi Y (2002) Otolith formation and endolymph chemistry: A strong correlation between the  
635 aragonite saturation state and pH in the endolymph of the trout otolith organ. *Mar Ecol Prog*  
636 *Ser* 231:237–245. doi: 10.3354/meps231237

637 Thomas ORB, Swearer SE, Kapp EA, Peng P, Tonkin-Hill GQ, Papenfuss A, et al (2019) The  
638 inner ear proteome of fish. *FEBS J* 286:66–81. doi: 10.1111/febs.14715

639 Tohse H, Ando H, Mugiya Y (2004) Biochemical properties and immunohistochemical  
640 localization of carbonic anhydrase in the sacculus of the inner ear in the salmon  
641 *Oncorhynchus masou*. *Comp Biochem Physiol - A Mol Integr Physiol* 137:87–94. doi:  
642 10.1016/S1095-6433(03)00272-1

643 Tohse H, Mugiya Y (2001) Effects of enzyme and anion transport inhibitor on in vitro  
644 incorporation of inorganic carbon and calcium into endolymph and otoliths in salmon  
645 *Oncorhynchus masou*. *Comp Biochem Physiol - A Mol Integr Physiol* 128:177–184.

646 Tohse H, Mugiya Y (2008) Sources of otolith carbonate: experimental determination of carbon  
647 incorporation rates from water and metabolic CO<sub>2</sub>, and their diel variations. *Aquat Biol*  
648 1:259–268. doi: 10.3354/ab00029

649 Tohse H, Murayama E, Ohira T, Takagi Y, Nagasawa H (2006) Localization and diurnal  
 650 variations of carbonic anhydrase mRNA expression in the inner ear of the rainbow trout  
 651 *Oncorhynchus mykiss*. Comp Biochem Physiol B Biochem Mol Biol 145:257–64. doi:  
 652 10.1016/j.cbpb.2006.06.011

653 Tresguerres M, Katoh F, Fenton H, Jasinska E, Goss GG (2005) Regulation of branchial V-H(+)-  
 654 ATPase, Na(+)/K(+)-ATPase and NHE2 in response to acid and base infusions in the Pacific  
 655 spiny dogfish (*Squalus acanthias*). J Exp Biol 208:345–54. doi: 10.1242/jeb.01382

656 Tresguerres M, Buck J, Levin LR (2010a) Physiological carbon dioxide, bicarbonate, and pH  
 657 sensing. Pflugers Arch Eur J Physiol 460:953–964. doi: 10.1007/s00424-010-0865-6

658 Tresguerres M, Levin LR, Buck J, Grosell M (2010b) Modulation of NaCl absorption by  
 659 [HCO<sub>3</sub><sup>-</sup>] in the marine teleost intestine is mediated by soluble adenylyl cyclase. AJP Regul  
 660 Integr Comp Physiol 299:R62–R71. doi: 10.1152/ajpregu.00761.2009

661 Tresguerres M, Parks SK, Salazar E, Levin LR, Goss GG, Buck J (2010c) Bicarbonate-sensing  
 662 soluble adenylyl cyclase is an essential sensor for acid/base homeostasis. Proc Natl Acad Sci  
 663 U S A 107:442–447. doi: 10.1073/pnas.0911790107

664 Tresguerres M (2014) sAC from aquatic organisms as a model to study the evolution of  
 665 acid/base sensing. Biochim Biophys Acta - Mol Basis Dis 1842:2629–2635. doi:  
 666 10.1016/j.bbadis.2014.06.021

667 von Biela V, Newsome S, Zimmerman C (2015) Examining the utility of bulk otolith  $\delta^{13}\text{C}$  to  
 668 describe diet in wild-caught black rockfish *Sebastes melanops*. Aquat Biol 23:201–208. doi:  
 669 10.3354/ab00621

670 Watanabe K, Ogawa A (1984) Carbonic anhydrase activity in stria vascularis and dark cells in  
 671 vestibular labyrinth. Ann Otol Rhinol Laryngol 93:262–266. doi:  
 672 10.1177/000348948409300315

673 Wilson JM, Randall DJ, Donowitz M, Vogl AW, Ip AK (2000) Immunolocalization of ion-  
 674 transport proteins to branchial epithelium mitochondria-rich cells in the mudskipper  
 675 (*Periophthalmodon schlosseri*). J Exp Biol 203:2297–2310.

676 Wilson JM, Whiteley NM, Randall DJ (2002) Ionoregulatory changes in the gill epithelia of  
 677 coho salmon during seawater acclimation. Physiol Biochem Zool 75:237–49. doi:  
 678 10.1086/341817

679 Zdebik AA, Wangemann P, Jentsch TJ (2009) Potassium ion movement in the inner ear: Insights  
 680 from genetic disease and mouse models. Physiology 24:307–316. doi:  
 681 10.1152/physiol.00018.2009

682  
 683  
 684

Fig 1

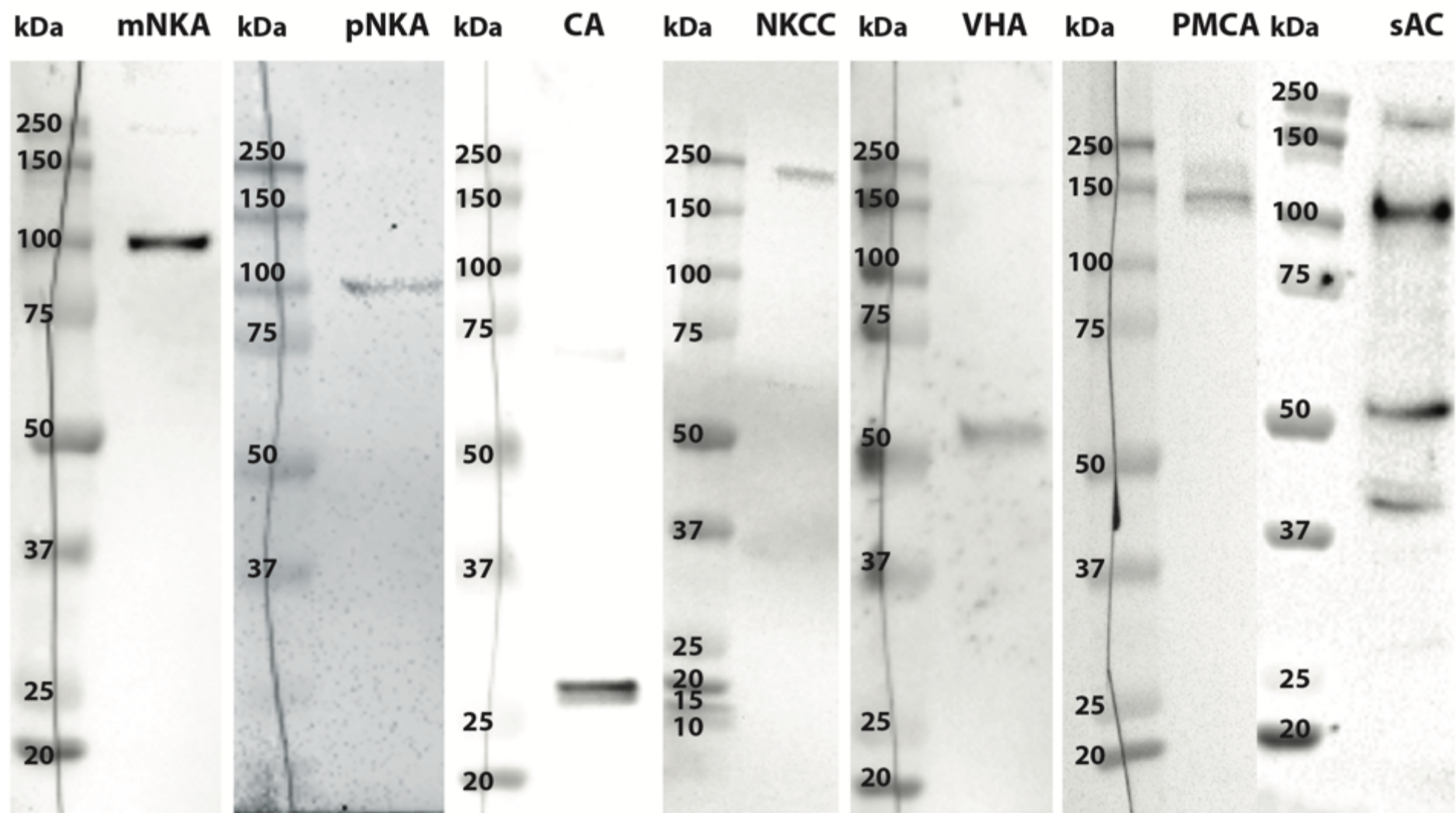


Fig 2

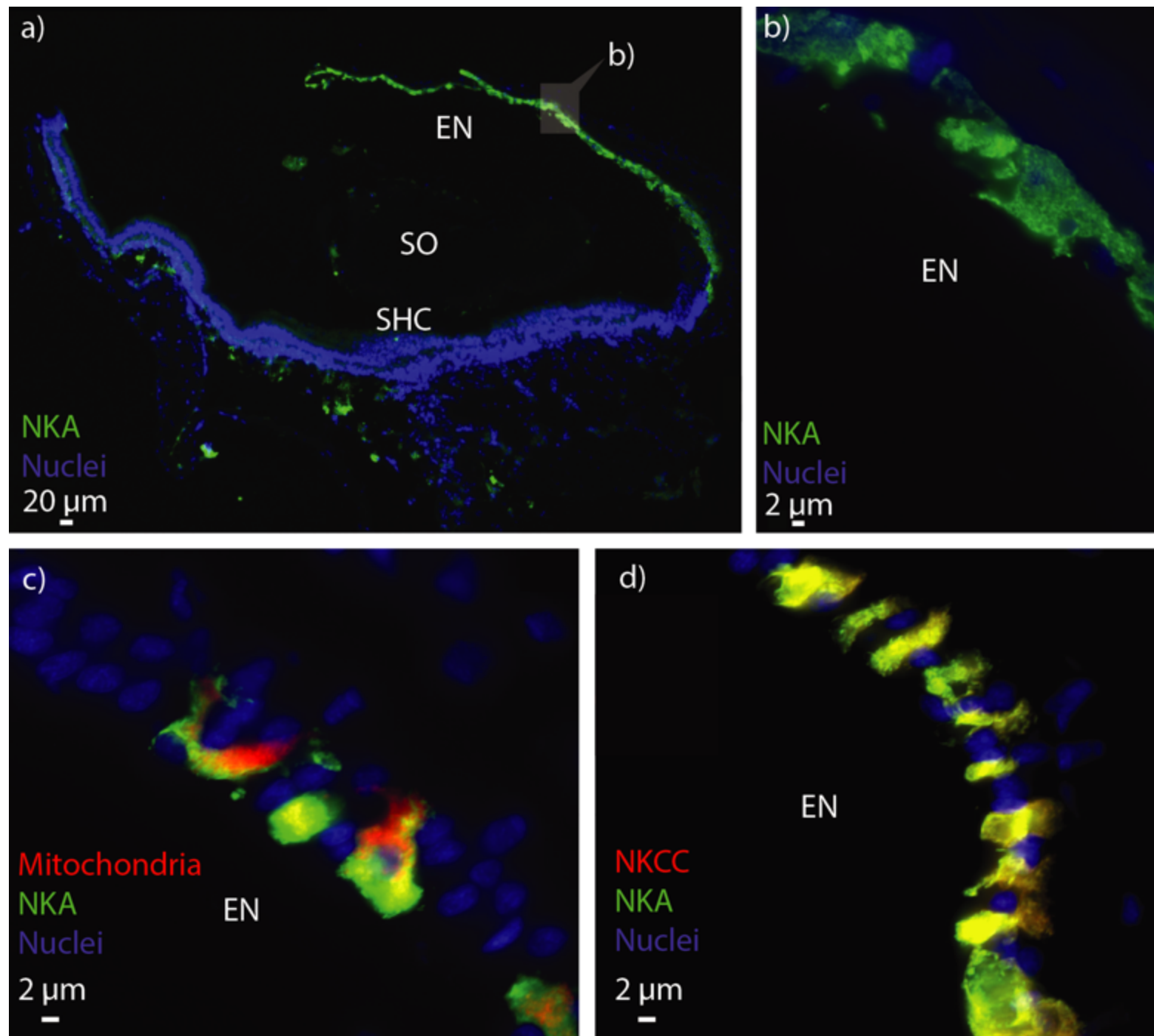


Fig 3

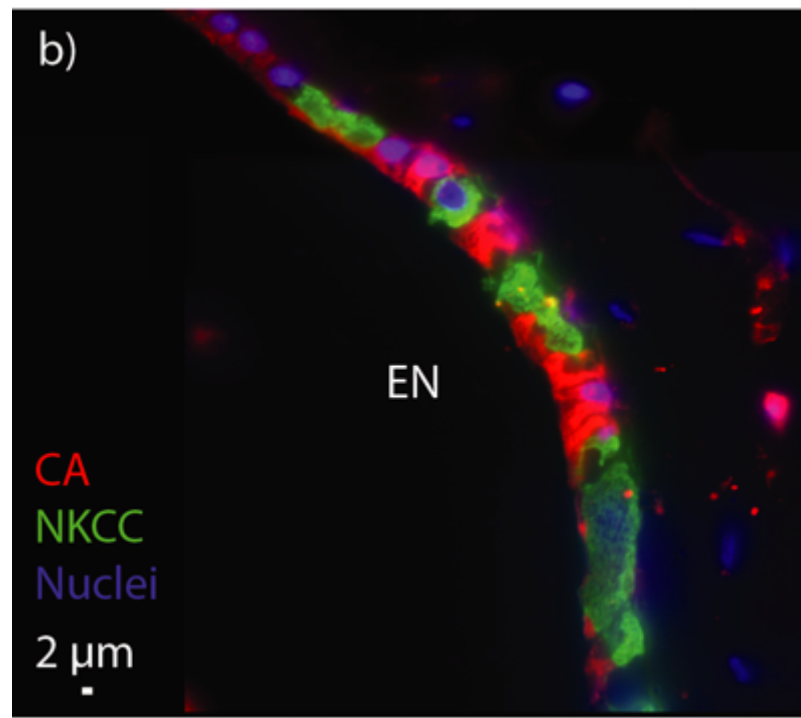
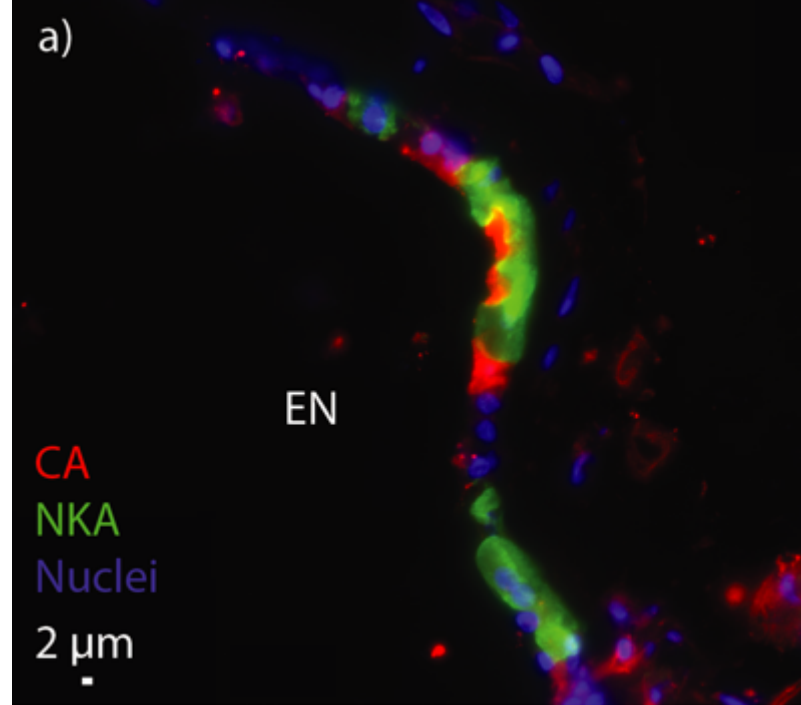




Fig 4

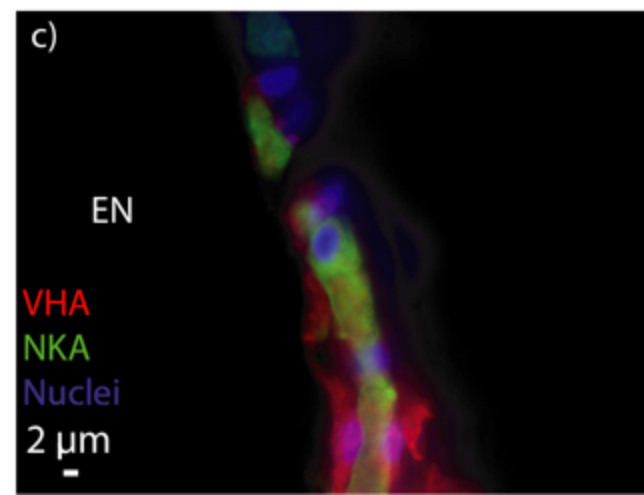
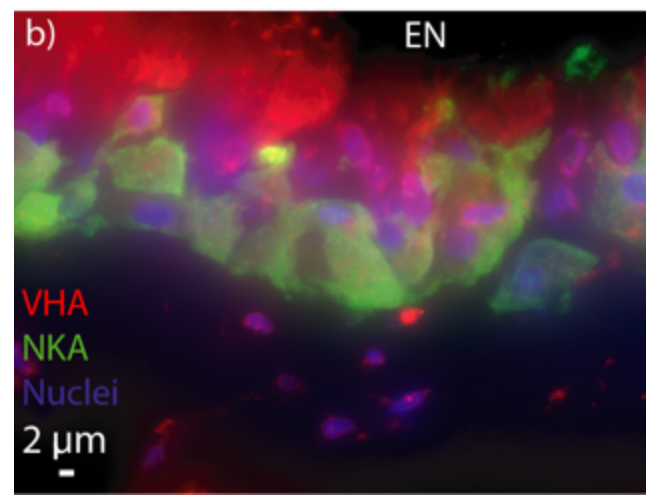
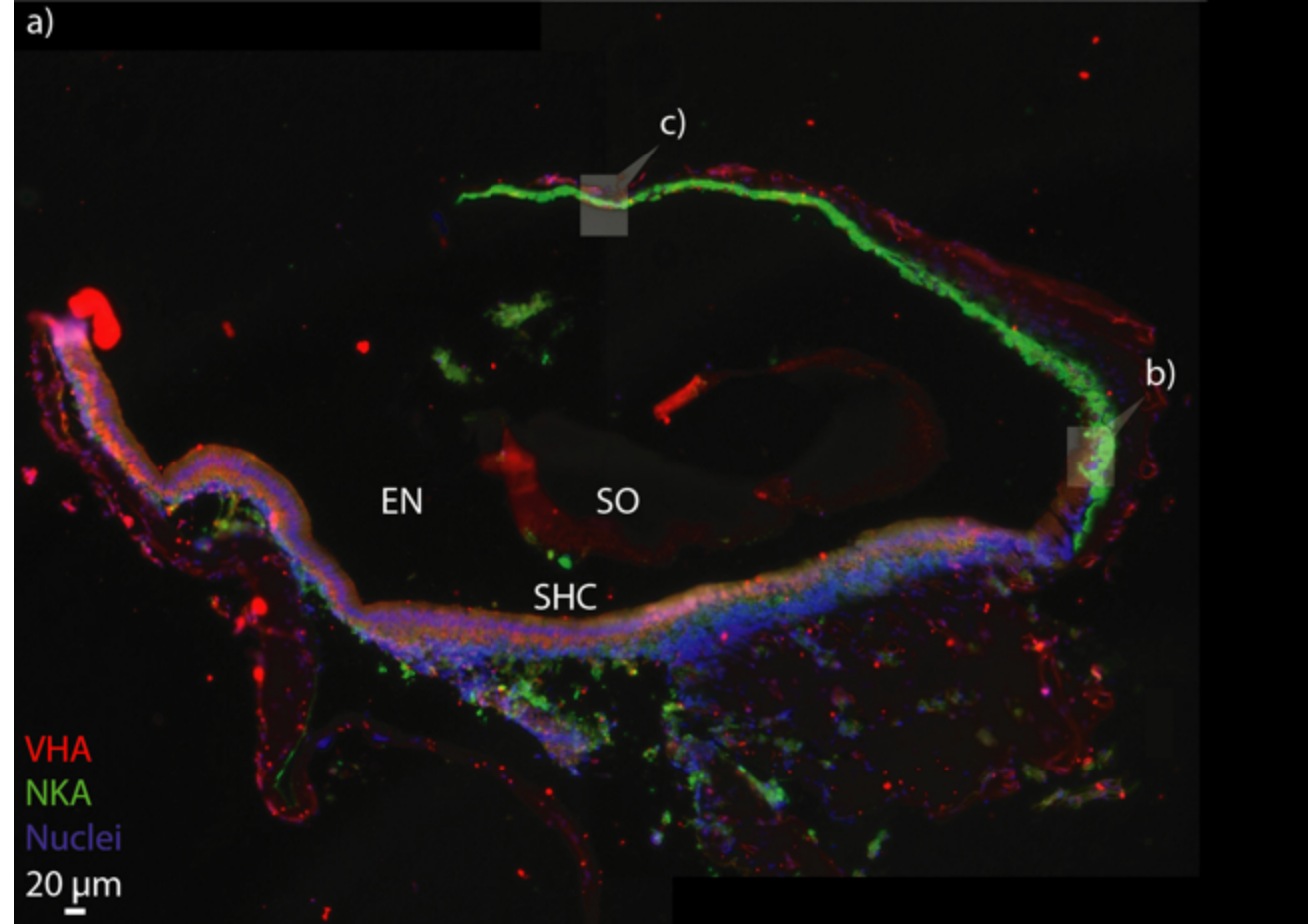


Fig 5

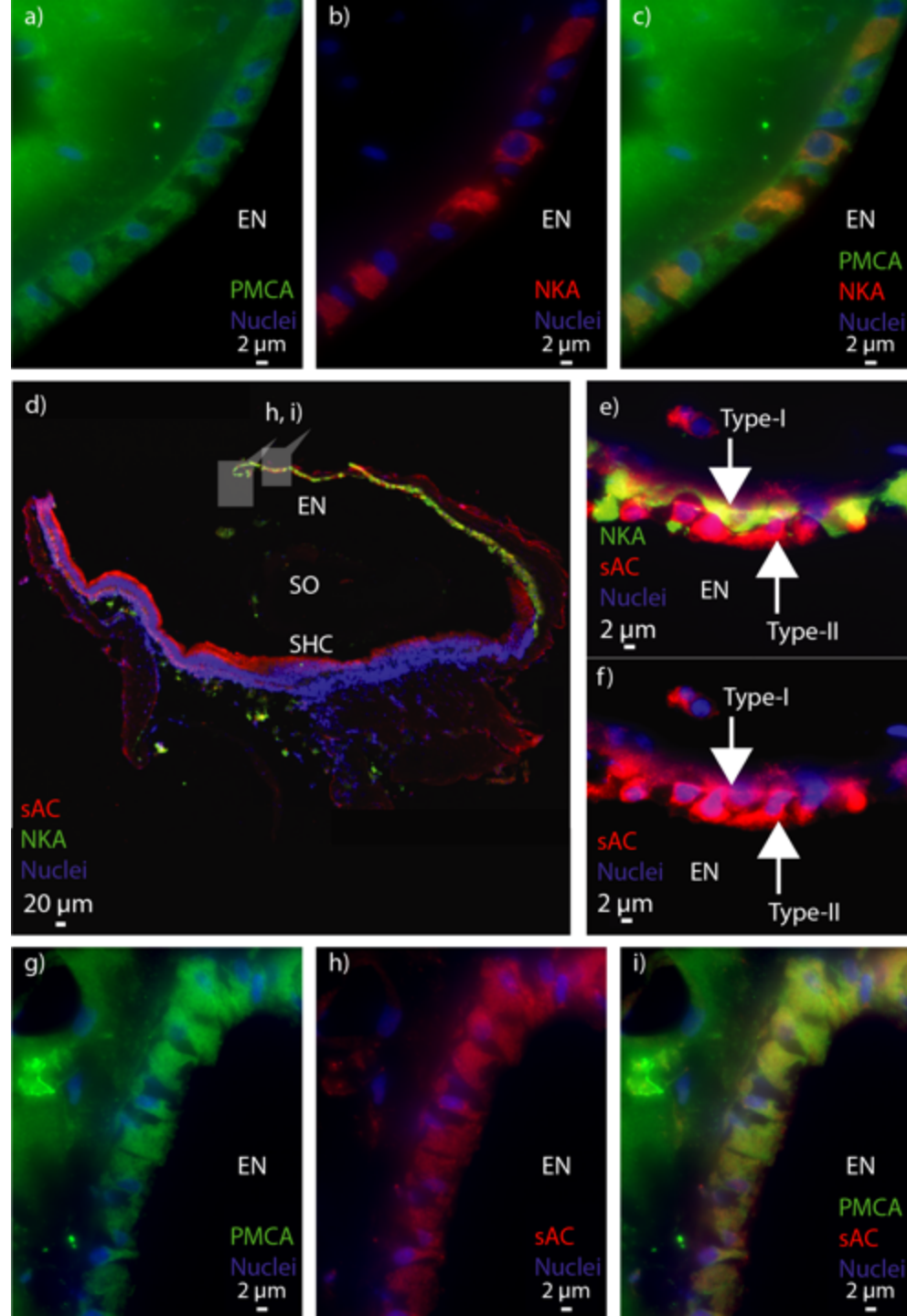


Fig 6

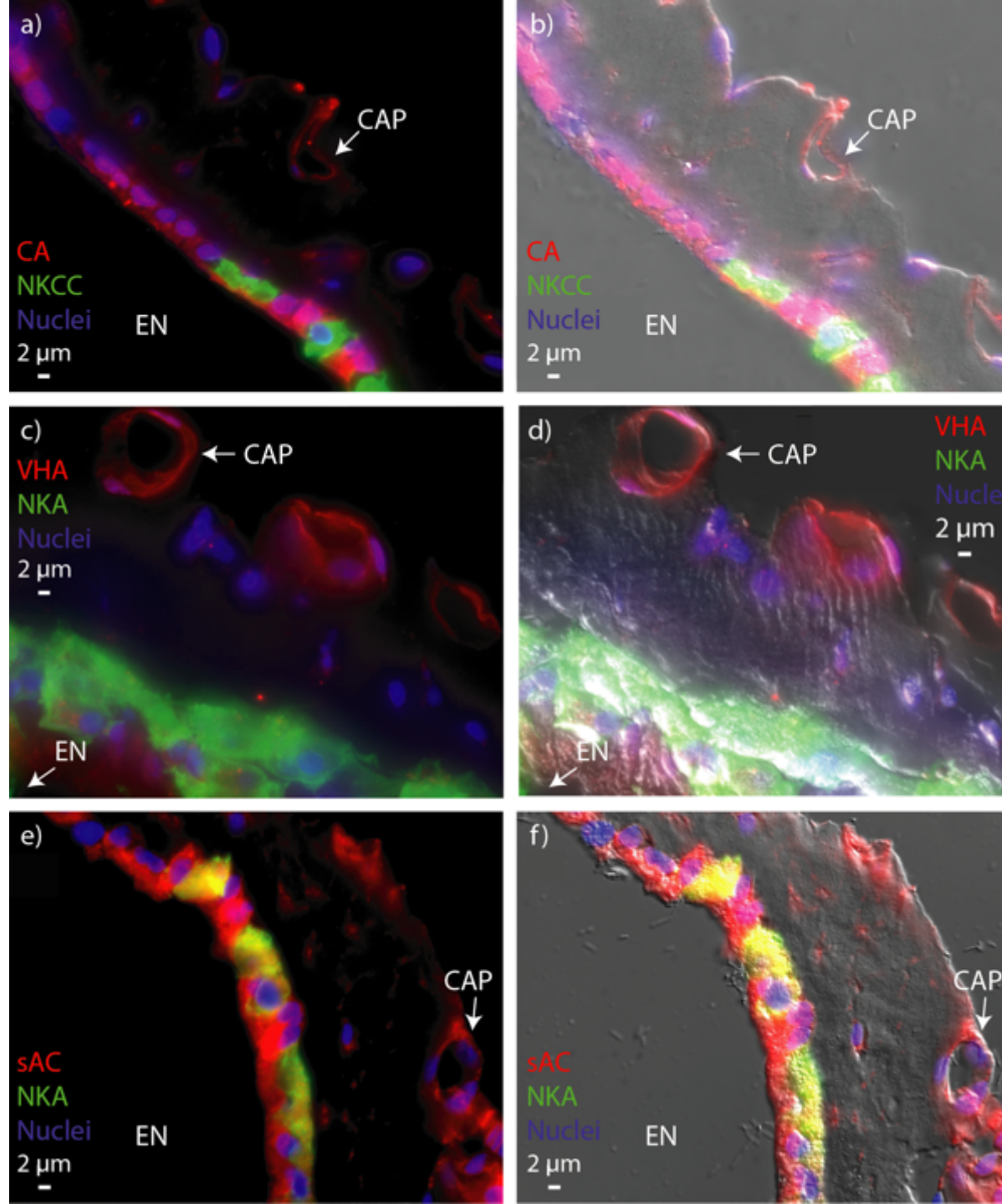


Fig 7

